Resilience-based post disaster recovery optimization for infrastructure system via Deep Reinforcement Learning

Huangbin Liang[1,*], Beatriz Moya[2,3], Francisco Chinesta[2,3], and Eleni Chatzi[1,4]

[1] Future Resilient Systems, Singapore-ETH Centre, CREATE campus, 1 CREATE Way, Singapore, 138602, Singapore;
[2] CNRS@CREATE LTD., CNRS, 1 CREATE Way, Singapore, 138602, Singapore;
[3] ENSAM Institute of Technology, 151 Bvd. de l'Hôpital, Paris, 75013, France;
[4] Department of Civil Environmental and Geomatic Engineering, ETH Zürich, Stefano-Franscini-Platz-5, Zurich, 8093, Switzerland;
∗ Corresponding email: huangbin.liang@sec.ethz.ch

Abstract. Infrastructure systems are critical in modern communities but are highly susceptible to various natural and man-made disasters. Efficient post-disaster recovery requires repair-scheduling approaches under the limitation of capped resources that need to be shared across the system. Existing approaches, including component ranking methods, greedy evolutionary algorithms, and data-driven machine learning models, face various limitations when tested within such a context. To tackle these issues, we propose a novel approach to optimize post-disaster recovery of infrastructure systems by leveraging Deep Reinforcement Learning (DRL) methods and incorporating a specialized resilience metric to lead the optimization. The system topology is represented adopting a graph-based structure, where the system's recovery process is formulated as a sequential decision-making problem. Deep Q-learning algorithms are employed to learn optimal recovery strategies by mapping system states to specific actions, as for instance which component ought to be repaired next, with the goal of maximizing long-term recovery from a resilience-oriented perspective. To demonstrate the efficacy of our proposed approach, we implement this scheme on the example of post-earthquake recovery optimization for an electrical substation system. We assess different deep Q-learning algorithms to this end, namely vanilla Deep Q-Networks (DQN), Double DQN(DDQN), Duel DQN, and duel DDQN, demonstrating superiority of the DDQN for the considered problem. A further comparative analysis against baseline methods during testing reveals the superior performance of the proposed method in terms of both optimization effect and computational cost, rendering this an attractive approach in the context of resilience enhancement and rapid response and recovery.

Keywords: Resilience · post-disaster recovery · deep reinforcement learning · deep Q-network · infrastructure systems.

1 Introduction

Infrastructure systems are vital for upholding societal and economical functionality within modern societies. They encompass a broad range of essential services, including power grids, transportation networks, water supply and communication networks, which collectively support the well-being and productivity of communities. However, these critical systems are highly vulnerable to a variety of natural and man-made disasters, such as earthquakes, floods, hurricanes, and terrorist attacks [15]. Such, often unforeseen, events cause disruptions within and even across such systems, leading to substantial economic loss and societal impact [6, 12]. In trying to optimally design these systems in anticipation of such adverse effects, a significant hurdle lies in the lack or limited amount of emergency repair resources. This renders extensive simultaneous repairs infeasible, which may prolong the recovery time and further exacerbate the adverse consequences [42]. The ability of infrastructure systems to quickly recover following disaster events, defined under the term of resilience, is a desired trait both in terms of design, as well as life cycle support of such extended networks. The latter necessitates efficient decision-making approaches that can maximize the use of available resources and ensure the fastest recovery path [22, 35, 54, 38].

The term resilience is widely used in infrastructure systems to describe the system's capacity to withstand and recover from disturbances or disruptions, and can be characterized under four main properties, i.e., robustness, rapidity, redundancy, and resourcefulness [2]. The resilience curve is often used to define the time evolution of the system's performance, forming an effective means to quantitatively measure a system's resilience against disasters [2, 4]. As illustrated in Fig. 1, the resilience curve captures the dynamic evolution of the system performance $F(t)$. The curve is characterised by a significant drop to a certain level F_d when a disastrous event strikes, and is gradually restored back to normal levels as the recovery efforts initiate and unroll. Noteworthy, the resilience curve is influenced by the choice of a specific performance indicator. Scholars have proposed different performance indicators for various infrastructure systems based on their network attributes and functional requirements [36, 39, 41], such as node satisfaction, network connectivity, traffic flow capacity, service supply capacity, travel time and more. Accordingly, infrastructure resilience can be quantified using residual functionality, recovery time, or alternate comprehensive metrics that can be obtained from the corresponding resilience curves. A commonly adopted resilience index is the so-called lack of resilience (LoR), which corresponds to the area between the time-dependent performance trajectory and the constant performance requirement F_0 during the entire recovery process, as represented in gray in Fig. 1 and computed by Eq.(1). Over the years, various frameworks and metrics have further been developed to quantify the resilience of infrastructure systems based on the characteristics of the resilience curve, evolving from deterministic to stochastic tools [51, 9, 32, 56], from focusing on a single to multiple hazards [7, 28], and from using a single, static metric to multi-dimensional, dynamic indicators [34, 66]. Still, the disaster resilience quantification considering the interrelated impacts and cascading failures of multiple systems at the urban scale deems further research for ensuring actionable implementation [30, 29, 57]. LoR is defined as follows:

$$LoR = \int_{t_0}^{t_1} [F_0 - F(t)]\, \mathrm{d}t, \tag{1}$$

where $F(t)$ represents the time-varying system performance, F_0 refers to the initial system performance, and t_0 and t_1 indicate the time instances when the disaster occurs and when the system performance completely recovers, respectively.

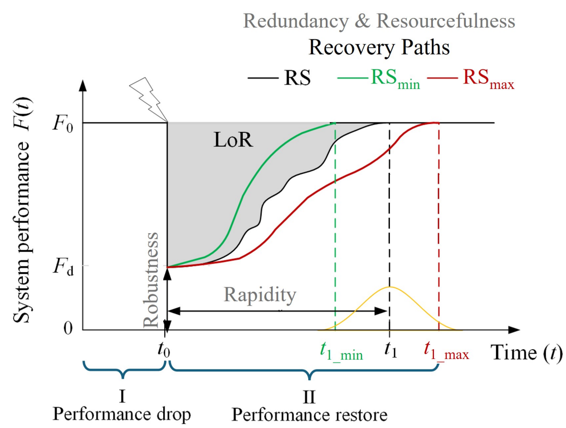

Fig. 1. Illustration of resilience curve in terms of infrastructure system performance, following different recovery strategies. In phase I, a performance drop is induced by a disturbance or disastrous event. The remaining capacity, or residual performance of the system, is termed robustness. In phase II, the performance is restored. Different recovery plans can be followed leading to different LoR. Redundancy represents the degree of substitute components of a system; Resourcefulness is the capacity to prioritize tasks and allocate resources effectively after a disaster; Rapidity is the capability to quickly respond and recover from disaster impacts to restore the desired performance level, and it will be greatly affected by Redundancy and Resourcefulness.

Considering the potentially large number of damaged components and the typically limited resources available for repair, the sequence in which infrastructure components are restored has a major impact on the efficiency of the recovery process. Given a fixed initial damage scenario, the choice of different recovery strategies can lead to different repair sequences and resilience curves, as displayed in Fig. 1. The performance curve-based resilience quantification framework allows to prioritize repair actions according to their impact on system functionality and resilience. The lower the LoR, the more resilient the system is and the faster the system recovers. Currently, various resilience-inspired methods have been developed to determine the optimal sequence for infrastructure restoration following a disaster, including static component ranking-based methods [33, 8], greedy evolutionary algorithms [16, 55, 68], and data-driven machine learning models [40, 11]. While these methods have made some progress in finding recovery strategies, they still suffer from considerable limitations in terms of effectiveness, robustness, adaptability, and scalability in handling complex real-world scenarios.

Component ranking-based methods prioritize the repair order based on predetermined criteria such as component importance or criticality. For instance, in the context of electrical substations, which will be employed as a use-case herein, components like transformers and circuit breakers may be ranked higher due to their critical role in power distribution [33, 46]. Some topological attributes like node degree and edge betweenness were also used as the criticality indicators in previous study [8, 27, 31, 61]. Accordingly, the sequence of repairing damaged components after a disaster is carried out according to a predetermined fixed order, with the most critical components being repaired first, then the less critical ones. These methods are straightforward and easy to implement, providing interpretable and transparent policies, which can be easily adopted for decision-making. However, they are not resilience-oriented and do not account for dynamic interactions and interdependence between components. This can lead to suboptimal recovery plans that do not fully restore system functionality in a timely manner.

Evolutionary algorithms iteratively explore the search space of possible repair sequences and greedily select the one that optimizes a predefined resilience-oriented objective, such as minimizing downtime or the introduced LoR. For example, the genetic algorithm (GA), tabu search algorithm, and simulated annealing (SA) are widely employed in the post-disaster recovery optimization of transportation networks and power systems [16, 55, 68, 3, 45, 18, 48]. While these methods can handle complex scenarios and dependencies, they often lack dynamic adaptability and struggle with high-dimensional search spaces, which can lead to increased computational demands and slower convergence. Additionally, their performance can be inconsistent and unstable, sometimes failing to find the global optimum due to their heuristic nature.

Data-driven machine learning models leverage simulation or historical data to learn patterns and relationships between infrastructure components in a supervised manner. Once trained, these are expected to provide timely decisions based on real-time damage assessment, as this stems from deployed measurement (monitoring) systems. Such sequence-to-sequence models have been successfully applied in applications related to path planning, supplier selection, and the traveling salesman problem [40, 21, 24, 11]. While promising for optimizing disaster recovery rapidly, their efficacy heavily depends on the quantity, quality and representivity of the training dataset (i.e., the input damage positions and the corresponding ground-truth output sequences). The challenge in obtaining such datasets is compounded by the fact that this optimization problem is NP-hard, meaning that generating sufficient and representative training data is computationally infeasible [1]. The NP-hard nature of the problem underscores the difficulty in ensuring that the dataset covers all the possible disaster situations that could happen, which is necessary to train models that can handle potential disaster scenarios effectively. Moreover, models trained on specific small-scale datasets may not generalize well to new or unseen scenarios, limiting their applicability and reliability in real-world disaster recovery optimization.

Reinforcement learning (RL) algorithms provide a further avenue for optimizing post-disaster repair sequences compared to supervised data-driven machine learning models that learn from fixed labeled input-output pairs, by interacting with a simulated environment and receiving feedback on the performance of different actions. They offer several advantages over traditional optimization methods. Firstly, RL inherits the foundational frameworks of dynamic programming and Markov decision processes (MDP), making it naturally suited for handling dynamic sequence optimization problems with strong theoretical support. Secondly, RL continuously learns and improves its policy through interactions with the environment, reducing the need for large hard-to-obtain labelled data. Thirdly, RL schemes provide a policy that can dynamically adapt to different scenarios, as it considers the current state of the environment and appropriately recommends a next action. This implies greater flexibility in accounting for diverse and uncertain disturbances as compared against traditional optimization methods. Fourth, RL alleviates the curse of dimensionality in high dimensional problems, finding solutions more efficiently than previous algorithms. Given these merits, a list of RL-based solutions have been developed and applied to the optimal inspection and management planning of infrastructures under long-term environmental deterioration [37, 58, 63, 20]. Despite the existence of some applications of RL in the case of infrastructure recovery after extreme disasters [67, 53, 52, 44], such methods experience hurdles in tackling previously unseen post-disaster environments, particularly in high-dimensional state-action spaces [36, 43]. Another critical issue lies in the design of the reward function, which is often not efficiently defined to reflect the true objectives of disaster recovery, such as balancing immediate functionality restoration with long-term resilience.

To address these issues, this paper proposes a resilience-based DRL approach for optimizing the post-disaster recovery of infrastructure systems s from the system's worst post-disaster damage state, which assumes that all components are damaged. This hypothesis serves as the initial environment, where exploration starts from. The recovery process is formulated as a sequential decision-making problem where the agent selects actions (i.e., determining which components to repair) to maximize expected long-term resilience outcomes. We employ Deep Q-learning algorithms because they are well-suited to handle the uncertainty and complexity of dynamic environments, particularly in scenarios with high-dimensional state and discrete action spaces. Deep Q-learning leverages deep neural networks to approximate the Q-value function that represents the expected cumulative reward of taking a particular action in a given state [10], allowing it to effectively manage high-dimensional state and action spaces where other methods may fail. Additionally, the stability of such schemes, enhanced by experience replay and target networks, ensures robust decision-making in dynamic environments. Compared to other reinforcement learning algorithms, Deep Q-learning excels in simplicity and generalization from limited experience, making it a more efficient and reliable choice for our task. By assuming the worst-case post-disaster damage, the agent learns to identify the most effective repair strategies to enhance the system's overall resilience with a wider and general vision for any potential combination of damaged equipment. The reward is defined based on resilience metrics. We leverage a reward function that draws explicit information on resilience from corresponding resilient curves [67, 53], and propose as a novel aspect the use of the LoR as the chosen resilience metric for this task, adapted to the proposed use case presented in this work. Besides, we describe the geometry of the use case following a graph-based approach to profit from the benefits of this characterisation. Graph abstractions enables modelling of complex dependencies, relationships and interactions between system components, such as the influence of topological structure on failure propagation [5]. In a DRL algorithm, this characteristic allows the agent to analyse and track actions more efficiently. In addition, the agent will be capable of handling possibly large, unstructured configurations where connections could be as important as the nodes themselves, leading to more accurate and scalable decision-making in dynamic recovery scenarios. Finally, for future digital twin developments, a graph approach enables the interaction between layers of information and comprehensive understanding of the system's behavior. Furthermore, we have equipped the proposed resilience-based DRL approach with modified action selection techniques to achieve agent action convergence, and action masks to penalize repeated actions, further improving its performance.

We demonstrate the functionality and efficacy of our proposed approach on the example of post-earthquake recovery optimization for electrical substation systems. Network and power recovery planning is crucial for ensuring rapid service restoration while employing a minimal number of resources. Examples rooted in recovery optimization of power and communication networks have previously appeared in the literature. In this vein, authors in [59] propose the use of hybrid digital twins based on a Bayesian Neural Network, monitored and updated in real-time, to connect the power network and the road network influence to simulate potential recovery strategies. Hosseini and Parvania [44] show an application of DRL to prevent power outages by efficient planning of power storage units. Akashi et al. [52] demonstrates use of DRL for predicting the optimal recovery sequence for telecommunication networks during earthquakes and typhoons, when equipment resources sustain damage as a result of structural collapse, inundation, or electrical outages. DRL has also been applied to electrical distribution networks to allow for reconfiguration to recover power supply [62, 50]. However, most DRL approaches typically focus on performance optimization, such as efficiency, speed, cost, or energy savings, without necessarily considering resilience explicitly. Furthermore, existing strategies are often pretrained on some random scenarios and still require further retraining or transfer learning when applied to an unseen environments [67], limiting their generalization and real-time decision-making capacities. The contributions of this paper are summarized as follows:

– We develop a resilience-based DRL sequential decision-making framework for substation recovery, using a graph-based representation of the network topology and proposing the *LoR* as the metric to lead the optimization. Unlike previous DRL works that often focus on static resource availability and performance optimization, this framework enables the agent to learn optimal repair strategies without requiring extensive labeled data, while accounting for specified resilience targets and dynamic repair resources.
– We propose a training strategy for the DRL-based model learning from the worst-case scenario to equip it with broader exposure to potential disruptions, enhancing its adaptability and robustness in responding to a wide range of unforeseen disaster scenarios without the need for retraining or further learning. In this strategy, a higher degree of generalization is reached with less training data.
– We provide a comparison of different DRL architectures and further compare the recovery solution derived by the best-performing architecture across various initial damage scenarios against the ground truth obtained from exhaustive enumeration, or baselines generated by genetic algorithms, demonstrating the superior performance of the proposed DRL-based approach in terms of both optimization effect and computational efficiency.

The paper is structured as follows. Section 2 briefly explains RL, deep Q-learning and its variants. The problem description and the proposed methodology are elaborated in Section 3 with an illustrated multi-input-multi-output(MIMO) system. Section 4 presents the practical case study and analysis results. Conclusions are drawn in Section 5.

2 Background

2.1 RL and Markov Decision Processes (MDPs)

RL is a branch of machine learning that focuses on addressing sequential decision-making problems by learning how agents should act within a particular environment to maximize some notion of cumulative reward. Unlike supervised learning, where the model learns from fixed labeled input-output pairs, RL learns from the consequences of actions, adjusting policies based on rewards and punishments. This trial-and-error learning paradigm makes RL suitable for a wide range of applications in complex environments, such as robotics, game playing, and autonomous systems [19]. The involved elements of RL and their interactions are depicted in Fig. 2 and defined as follows:

- Agent: the decision maker that interacts with the environment.
- Environment: everything external to the agent. The environment provides the context within which the agent operates and responds to the agent's actions by transitioning between states and providing rewards.

- State/Observation: a representation of the current situation or context that contains all the information necessary to make decisions.
- Action: the set of all possible moves or decisions the agent can make. Each action taken by the agent can lead to different states and rewards.
- Reward: the feedback from the environment as a result of the agent's actions.

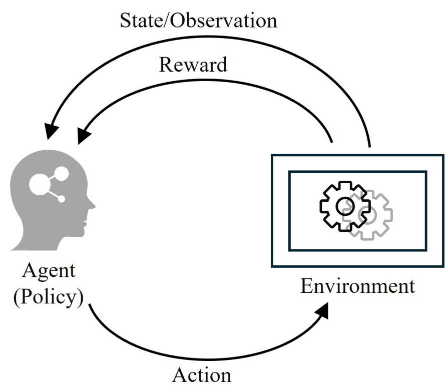

Fig. 2. RL elements and interactions

RL relies on the framework provided by Markov decision processes to effectively solve sequential decision-making problems. An MDP, usually characterized by a discrete time step-wise 4-tuple $[\mathcal{S}, \mathcal{A}, P(s_t, s_{t+1}, a_t), R(s_t, s_{t+1}, a_t)]$, offers a formal way to describe the dynamics of the environment. Here, $\mathcal{S}$ and $\mathcal{A}$ represents the set of possible states and actions respectively, and $s_t, s_{t+1} \in \mathcal{S}; a_t \in \mathcal{A}$. The term $P(s_t, s_{t+1}, a_t)$ indicates the probability of transitioning from state s_t to state s_{t+1} when action a_t is performed. $R(s_t, s_{t+1}, a_t)$ is the reward function that provides an immediate reward r_t from the environment when transitioning from s_t to s_{t+1} under action a_t at each time step. In this context, the RL goal is to develop a policy, denoted as π, that maps states to actions for each time step (i.e., $a_t = \pi(s_t))$) in a way that can eventually maximize the cumulative reward over the long run, as presented by Eq.(2). Accordingly, the policy that maximizes the expected cumulative future reward $Q_\pi(s, a)$ in Eq.(3) is referred to as the optimal policy π^*. It should be noted that both the state-transition probability $P(s_t, s_{t+1}, a_t)$ and the reward function $R(s_t, s_{t+1}, a_t)$, are intrinsic properties of the environment and are typically unknowable in practice. Thus, the optimal policy π^* is learned exclusively through the agent's interactions with the environment utilizing specific learning algorithms.

$$G_t = r_t + \gamma \times r_{t+1} + \gamma^2 \times r_{t+2} + ... = \textstyle\sum_{k=0}^{\infty} \gamma^k \cdot r_{t+k}, \tag{2}$$

$$\begin{aligned} Q_\pi(s, a) &= \mathbb{E}\left[G_t | s_t = s, a_t = a, \pi\right], \\ Q^*(s, a) &= Q_{\pi^*}(s, a) = \max_\pi Q_\pi(s, a), \end{aligned} \tag{3}$$

where G_t is the cumulative reward (also known as the return) from moment t; $\gamma \in [0, 1]$ denotes a discount factor that balances the significance of future rewards against immediate ones; $Q_\pi(s, a)$ is the Q-value function (also known as action-value function) that estimates the expected return of taking a particular action a in a given state s and following a particular policy π thereafter.

2.2 Q-Learning, Deep Q-network (DQN) and its variants

Q-Learning is a model-free and off-policy RL algorithm that aims to find the optimal policy by learning the Q-values for state-action pairs based on the agent-environment interactions. The Q-Learning update is recursively driven by the Bellman equation:

$$\hat{Q}_{k+1}(s, a) \leftarrow \hat{Q}_k(s, a) + \eta \left[r + \gamma \cdot \max_{a'} \hat{Q}_k(s', a') - \hat{Q}_k(s, a) \right], \tag{4}$$

in which $\hat{Q}$ represents an estimate of the Q-value; k denotes the number of iterations; η corresponds to the learning rate; r is the reward received after taking action a in state s; $\max_{a'} Q(s', a')$ stands for the maximum Q-value for the next state s'. Through iterative updates, Q-Learning converges to the optimal Q-values $Q_{\pi^*}(s, a)$, allowing the agent to derive the optimal policy by carrying out a greedy action that yields the highest value, i.e., $a = \operatorname{argmax}_a [Q_{\pi^*}(s, a)]$.

While Q-Learning is efficient for simple environments with a limited number of states and actions, it struggles with large discrete or continuous state spaces. This is where Deep Q-Learning, or Deep Q-Networks (DQN), comes into play. DQN extends Q-Learning to handle complex environments with large state/action spaces by using a deep neural network (DNN) to approximate the Q-value function [10, 17]. Instead of maintaining a tabular Q-values, a neural network (referred to as the policy Q-network) takes the state as input and outputs Q-values for each possible action. Two important techniques employed in DQN [10] are experience replay, where past experiences are stored and randomly sampled for training, and target networks, which stabilize training by providing consistent Q-value targets (Eq.(5)). These advancements break the correlation between consecutive experiences and lead to more stable learning. Then the policy Q-network is updated to minimize the difference between the predicted Q-value and the target Q-value through Eq.(6):

$$y = r + \gamma \cdot \max_{a'} Q^t(s', a'; \theta^-), \tag{5}$$

$$\begin{aligned} L(\theta) &= \mathbb{E}\left[(y - Q^p(s, a; \theta))^2 \right], \\ \theta &= \theta - \eta \cdot \bigtriangledown L(\theta), \end{aligned} \tag{6}$$

where θ are the parameters of the policy Q-network Q^p; θ^- represent the parameters of the target Q-network Q^t, which are updated periodically to match the Q^p. Here, the same network Q^t is used to select and evaluate actions, leading to a potential overestimation of Q-values.

Double Deep Q-Learning (DDQN) was introduced to address this overestimation issue by using two separate networks: one for selecting actions and the other for evaluating these. Thus, the target value in DDQN is computed differently from Eq.(5) to avoid the overestimation bias, given by Eq.(7) [13]:

$$y = r + \gamma \cdot Q^t(s', \underset{a'}{\operatorname{argmax}} Q^p(s', a'; \theta); \theta^-), \tag{7}$$

where the next action $\underset{a'}{\operatorname{argmax}} Q^p(s', a'; \theta)$ is selected using the policy network, and its corresponding Q-value is evaluated using the target network.

The dueling network architecture is another enhancement to the vanilla DQN by splitting the output into two streams that separately estimate the state-value, $V(s)$, which represents the overall value of being in a given state, and the so-called advantages, $A(s, a)$, which quantify the benefit of taking a specific action versus other actions in that state. These two estimates are then combined to produce the Q-values through the following equation [14]. The dueling network architecture is mentioned here because, in the following illustrative case study, we conduct a fair comparison between the vanilla DQN and several of its variants, including the Dueling architecture.

$$Q(s, a; \theta, \alpha, \beta) = V(s; \theta, \beta) + \left(A(s, a; \theta, \alpha) - \frac{1}{|\mathcal{A}|} \sum_{a'} A(s, a'; \theta, \alpha) \right), \tag{8}$$

in which θ denotes the parameters of the shared neural network layers, while α and β are the parameters of the two streams of fully-connected layers.

DQN and its advanced variants, such DDQN, Duel DQN, and Duel DDQN have demonstrated remarkable success in various domains [23, 25, 49, 64, 60, 52]. Their capability to handle complex, high-dimensional environments is promising in optimizing post-disaster infrastructure recovery, which is inherently characterised by uncertainty, offering a potential solution to infrastructure resilience enhancement.

3 Methodology

3.1 Overview

In practical terms, the problem we here wish to solve is to determine the optimal post-disaster recovery policy for a disaster-affected infrastructure network, with the aim of enhancing resilience, i.e., the return to equilibrium. This can be formulated as a sequential decision-making process, which aims to specify which damaged component(s) to repair at each time step based on the available resources and the current state of the infrastructure to maximize some metric of system-level resilience. We propose to derive such a resilience-targeted optimal recovery policy using a DRL-based decision support framework, as shown in Fig. 3. This framework comprises four key blocks:

1. Environment representation and network modeling,

2. Agent construction and action selection,
3. Resilience-oriented reward definition, and
4. Q-value update algorithm.

For simplification and without loss of generality, the detailed introduction of the involved blocks is illustrated through a representative MIMO substation system composed of five pieces of equipment, as seen in Fig. 4(a). Through these blocks, we will highlight the proposed algorithm enhancements and generalization training conditions, including the worst-case scenario initial training hypothesis, action mask techniques, and the improved action selection for agent convergence.

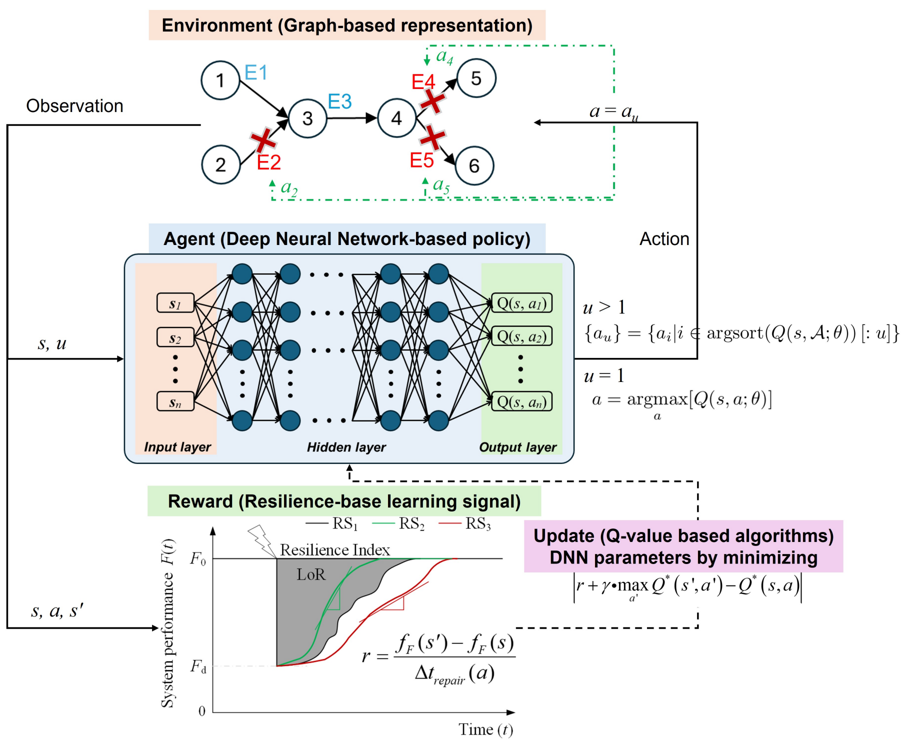

Fig. 3. Schematic diagram of the resilience-based post-disaster recovery optimization of infrastructure systems within a DRL-based decision support framework

3.2 DRL-based decision support framework components

Environment representation and equipment network modeling refers to accurately representing the post-disaster environment state and modeling the

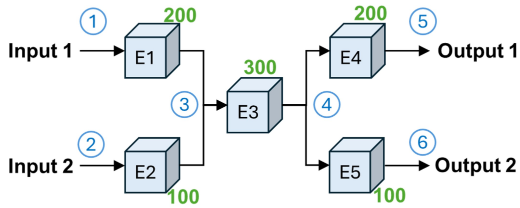

(*a*)

		To					
		1	2	3	4	5	6
From	1	0	0	E1	0	0	0
	2	0	0	E2	0	0	0
	3	0	0	0	E3	0	0
	4	0	0	0	0	E4	E5
	5	0	0	0	0	0	0
	6	0	0	0	0	0	0

(*b*)

Fig. 4. (a) Representative MIMO infrastructure system: the green text denotes the load capacity of each equipment, the blue circles number the nodes; (b) adjacency matrix describing the system topology and components interrelationship

infrastructure network system. The system environment information typically includes the current condition of infrastructure components s and their functional interdependencies, as well as the repair resource units u that are available to the decision-maker. Given the number of involved components n, the environment state can be captured by a vector with a length equal to n, i.e., $s = (s_1, s_2, ..., s_n)$, and $s_i \in \{ds_1, ds_2, ..., ds_l\}$ where ds_i denotes one of the damage states. To enhance computational efficiency and for simplifying the decision-making problem, a binary state assumption is often applied in representing the post-disaster damage scenario of infrastructure components. In this case, $s_i \in \{0, 1\}$ with 0 and 1 indicating damaged and operational state, respectively. In this respect, a repair action effectively means turning a 0 state to 1.

On the other hand, the graph theory is employed to construct the infrastructure system model composed of distributed components. For the illustrative MIMO system of Fig. 4(a), after labeling the nodes with numbers, its network topology can be displayed using a graph-based representation with six vertices, representing the connections among equipment, and five edges that represent the equipment elements (Fig. 3). Accordingly, an adjacency matrix A that describes the components' interdependencies within the network can be derived, as presented in Fig. 4(b), where the element $a_{ij} = 1$ if there is a directed edge from vertex i to vertex j; otherwise $a_{ij} = 0$; and under the binary state assumption Ei here determines the connectivity between two vertices based on the damage state of the equipment s_i. Accordingly, a corresponding connectivity matrix C that records all the reachability information of any two vertices can be obtained by Eq.(9). The system functionality, which is elaborated in the subsequent section, can be computed based on this generated C matrix given the current state vector s. The details of the graph transformation for network analysis have been described in [46].

$$C_{v\times v} = A_{v\times v} + A^2_{v\times v} + ... + A^v_{v\times v}, \tag{9}$$

where v represents the number of vertices in the directed graph of the system.

DRL agent construction and action selection are pivotal for learning an optimal recovery policy. In view of the large number of damage state combinations, the DRL agent employs a DNN that consists of input, hidden, and output layers, to approximate the Q-value function $Q(s, a; \theta)$. The input layer receives the state vector s and available resource units u at each time step; the multiple fully connected hidden layers process the input features to extract the complex relationships and dependencies in the data; the output layer provides the estimated Q-values for the agent's potential repair actions.

Additionally, the action mask technique is applied by setting Q-values of invalid actions (i.e., those that attempt to repair components that are either undamaged initially or have already been repaired) with a large negative value (e.g., $-inf$), to ensure that the derived repair strategy is practical and efficient. For instance in the MIMO substation system, let a_i denote the deployment of a repair resource unit to a specific damaged component Ei to carry out repair work, and suppose components $\{\mathrm{E2}, \mathrm{E4}, \mathrm{E5}\}$ are damaged, then the possible set of actions at this time step is $\mathcal{A} = \{a_2, a_4, a_5\}$, as depicted in Fig.3. Thus given the current state s and resource units u, the optimal action set $\{a_u\}$ can be selected by using a greedy policy in terms of the Q-values, mathematically represented as:

$$\{a_u\} = \{a_i | i \in \operatorname{argsort}(Q(s, \mathcal{A}; \theta))\,[: u]\}\,, \tag{10}$$

where the operation $\operatorname{argsort}(Q(s, \mathcal{A}; \theta))\,[: u]))$ returns the indices of the top u repair actions sorted by their Q-values. In this presentation, we apply the most simple case, where $u = 1$; we have a single agent that can repair a single piece of equipment at a time. Thus, the formula simplifies to selecting the single action with the highest Q-value, namely, $a = \underset{a}{\operatorname{argmax}}[Q(s, a; \theta)]$.

Resilience-oriented reward definition is about defining the reward function that guides the agent toward achieving the goal of enhanced system resilience. Reward metrics should be designed to reflect the improvement in resilience resulting from the agent's actions, with a larger positive reward assigned for the action that can lead to a quicker recovery of the system functionality. In this regard, the ratio of the system functionality improvement after completing a specific repair action over the duration of that action $\triangle t_{repair}(a)$ is adopted as the reward function, as presented by Eq.(11). It is noted that, in this case, the repair time for each equipment is assumed to be the same and defined as one-time unit for illustration, which can be conveniently replaced with other values. The reward function thus corresponds to the time-dependent slope of the performance-based resilience curve shown in Fig. 3.

$$r = \frac{f_F\left(s'\right) - f_F\left(s\right)}{\triangle t_{repair}\left(a\right)}, \tag{11}$$

where f_F denotes the one-to-one mapping function between the system's functionality and the components' state, as formulated in Eq.(12). In this study, the maximum allowable transmission capacity from the input terminals to the output terminals was defined as the functionality metric of the substation system, which takes the minimum of the total power input P_I, total power transformation P_T, and total power output P_O. These items are further computed by summarizing the accessible load capacity LC of the intact equipment in each section as below.

$$\begin{aligned} F &= f_F(s) = \min\left(P_I, P_T, P_O\right) \\ P_I &= s_1 \times LC_{E1} + s_2 \times LC_{E2} \\ P_T &= s_3 \times LC_{E3} \\ P_O &= s_4 \times LC_{E4} + s_5 \times LC_{E5} \end{aligned} \tag{12}$$

in which LC_{Ei} denotes the load capacity of each equipment, as provided by the green texts in Fig. 4 for the representative MIMO system.

Q-value parameters update ensures that the agent continuously improves its decision-making policy by learning from its iterative interactions with the environment, and this can be performed using different Q-value-based algorithms. The comprehensive comparison between the different state-of-the-art deep Q-learning algorithms is carried out for the practical case study in Section 4. Here, we detail the vanilla DQN process to optimize the post-disaster repair sequence of damaged components within the representative MIMO system recovery environment as an illustration, and the flowchart is displayed in Fig. 5:

1. set up all the relevant parameters, including those for tuning the epsilon changes in the dynamic $\epsilon-$greedy policy ($\epsilon_{start}, \epsilon_{end}, \epsilon_{decay}$), structures and weights of the policy Q network (θ) and target Q network (θ^-), the size of the replay memory (D) and training batch (n), the discount factor (γ), the leaning rate (η), the update frequency (K) and the number of episodes (N).
2. initialize the environment of the representative MIMO system with the most adverse damage state where all the equipment components were assumed to be damaged, because the worst-case scenario presents the greatest challenge to the algorithm, exposing it to the most complex and varied decision contexts during training [47]. This enhances the algorithm's adaptability, allowing it to handle various uncertain real-world post-disaster scenarios.
3. select an action at each time step based on a linearly changing epsilon value with respect to the episode number to balance exploration and exploitation, i.e., $\epsilon = \epsilon_{start} - \frac{\epsilon_{start} - \epsilon_{end}}{\epsilon_{decay}} \times episode$, with probability ϵ randomly select an action (exploration); otherwise select the action with the highest Q-value predicted from the policy Q network (exploitation) following Eq.(10).
4. implement the selected repair action a in the environment; record the required time and observe the resulting next state s'; calculate the system functionality by Eq.(12) as well as the instant reward r by Eq.(11); store the transition tuple (s, a, r, s') in the experience replay pool. Once the calculated system functionality recovers to the pre-disaster level, this episode is done,

and the corresponding LoR and return for this episode can be obtained by Eq.(1) and Eq.(2), respectively.

5. sample a batch of n transitions $\{(s_i, a_i, r_i, s_i')\}_{i=1,\dots,n}$ randomly from the memory pool when the number of the stored tuples is larger than n. Then for each transition, compute the target Q-value using the target Q network by Eq.(5), and perform a gradient descent step on the loss function to update θ through Eq.(6) with Adam optimizer.
6. update the weights of the target Q network to match the weights of the policy Q network every K time steps: $\theta^- \leftarrow \theta$. This helps in stabilizing the learning process by keeping the target values relatively stable over multiple updates.
7. repeat steps 2 to 6 for a predefined number N of episodes. Each episode represents a full post-disaster recovery rollout, containing a trial repair sequence; this strategy mimics an export accumulating experience as the trial-and-error process progresses.

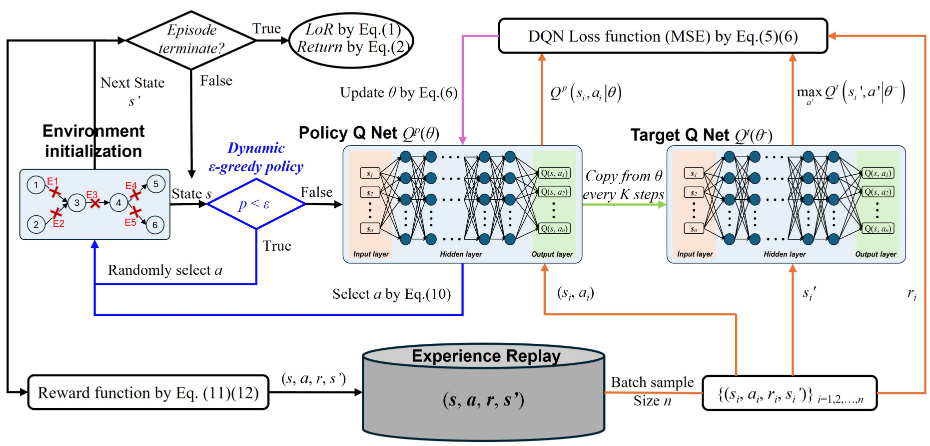

Fig. 5. DQN algorithm flowchart in the context of optimizing the repair sequence of components for the post-disaster system recovery environment

By following this detailed DQN algorithm process with appropriate parameter settings, the trained policy Q network model is expected to inform sequential repair actions based on the available resource units and the varying damage states, thereby forming a repair sequence that can enhance the system's overall resilience, as demonstrated below.

3.3 Results

The introduced DRL-based decision support framework is first implemented to optimize the repair sequence of damaged equipment in the representative MIMO system according to the blocks and process described in Section 3.2. Table 1 lists the hyperparameters used in the DQN algorithm, which are systematically tuned using a greedy search approach on this task. The performance of the proposed method across the training is presented in Fig. 6. Fig. 6(a) shows the rewards vary significantly with some low values at the beginning, but as training progresses, the rewards increase and stabilize after around 200 episodes due to the improvements in the agent's predictions for Q-values, as indicated by the decreasing loss in Fig. 6(b). Fig. 6(c) depicts the defined resilience index (LoR in Eq.(1)) based on the repair decisions by the DRL-based model during training episodes, with high initial fluctuations that diminish over time, suggesting the agent's growing effectiveness in enhancing system resilience as training advances. In the end, LoR is almost constant at the lowest value, indicating that the obtained repair policy is optimal for deciding the equipment repair orders for the damaged system. Moreover, this trend coincides with the reward changes, which demonstrates that the designed reward function is well-aligned with our target to enhance the system's overall resilience.

The agent model that achieved the best LoR outcome during training is stored for future application in any stochastic damage scenario. This model selects the most informed repair action that returns the highest Q-value at each time step based on the current input state until the system's functionality is fully restored. The generated repair sequence and resulting resilient curve can be obtained through recurrent updates to component states and system functionality from a certain initial damage scenario, as shown by the blue curves across different damage scenarios on the right side of Fig. 7. This figure also shows all the possible resilience curves in grey by enumerating all the possible permutations of the damaged components, with the best resilience curve among them highlighted in green dash for each provided damage scenario. Noteworthy, in some cases several pieces of equipment need to be repaired before an electrical transmission path can be reestablished so that the system's transmission capacity can be increased. Thus, different repair orders can produce the best resilience curve with the minimum LoR regardless of the priority of repairing the equipment involved in such electrical paths. For instance in Fig. 7(d), where E2, E4, and E5 were assumed to be damaged initially, following the repair orders of $(4, 2, 5)$ or $(4, 5, 2)$ listed in the left can both lead to the best recovery performance in Fig. 7(d). For the sake of brevity, they are denoted as $E4 \rightarrow (E5 \rightarrow E2)$, where the equipment repair order in the bracket can be shuffled and rearranged without affecting the final result. The ground truth by exhaustive search and the generated results from the trained model are perfectly matched in terms of both the optimal repair sequences and the resulting resilience curves, across both the training damage scenario and some random damage scenarios. This demonstrates the accuracy, efficiency, and adaptability of the introduced DRL-based decision support framework to provide the optimal repair sequence solution for infrastructure systems in the context of future post-disaster challenges. These are the main advantages of the model trained on the worst-case scenario, which can be applied to any damage scenario and generate excellent solutions without retraining.

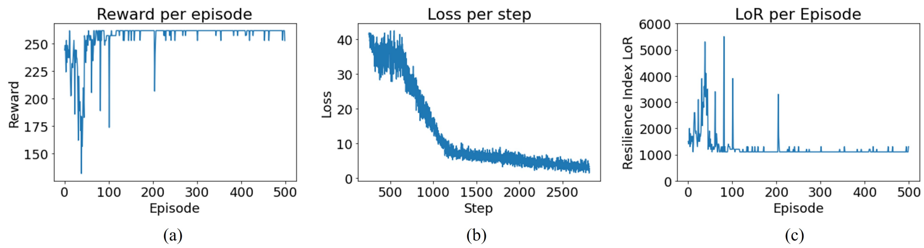

Fig. 6. Learning curves during training (a) Reward during training episodes; (b)Loss during training steps; (c) LoR during training episode

Table 1. Parameters for the training in the context of the illustrated MIMO system

Parameter	**Value**
Initial value of epsilon (ϵ_{start})	0.9
Final value of epsilon (ϵ_{end})	0.05
Number of episodes over which epsilon is linearly decayed (ϵ_{decay})	100
Dimension of state/action ($\mathcal{S}, \mathcal{A}$)	5
Number of hidden layer (n_{layer})	1
Number of neurons ($n_{neurons}$)	32
Size of replay memory (D)	10000
Batch size (n)	256
Discount factor (γ)	0.95
Learning rate (η)	0.001
Target Q network update frequency (K)	50
Number of episodes for training (N)	500

4 Practical Case Study

This section implements the introduced method to a real-world 220 kV substation system in an effort to investigate the scheme's robustness and scalability in providing an optimized recovery plan following an earthquake.

4.1 Substation environment description

Electrical substations play a vital role in the power transmission and distribution of a power system, featuring multiple input sources and output loads, sophisticated interconnections in parallel and series configurations, and a high

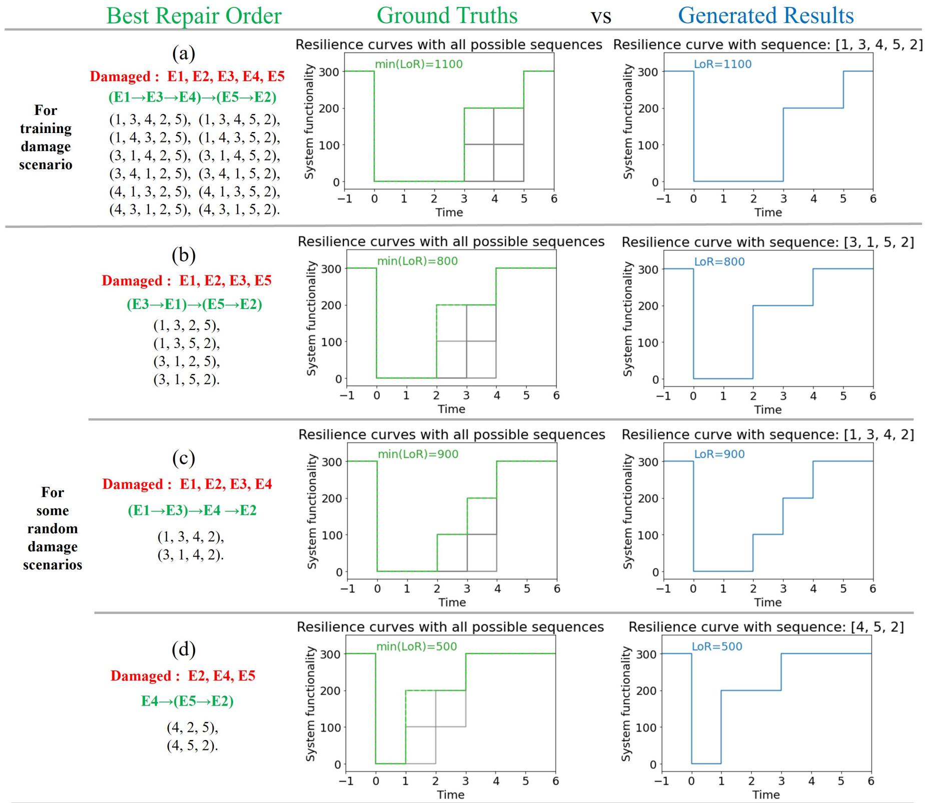

Fig. 7. Comparison in terms of the optimal repair orders and the resulting resilience curves between the ground truth by exhaustive search and the generated results from the trained model for (a) the training damage scenario; and (b)(c)(d) some random damage scenarios

degree of redundancy design in components. These features make the substation a complex and redundant system, serving as an excellent example to test the proposed method. Fig. 8 depicts the layout and composition of a practical 220 kv voltage step-down substation system, which mainly consists of three parts: electricity enters from the transmission lines to the 220 kV high voltage part, then goes through the voltage transformation part, and finally outputs to the power grid via the 110 kV low voltage part. As shown, there are a total of three 220 kV power input bays, three power transform bays, and six 110 kV power output bays arranged horizontally in the substation, and the adjacent double bus systems link them in a vertical arrangement, which are composed of two segments with a coupling bay to increase its reliability. Note that a substation contains hundreds of various types of electrical equipment, such as circuit breakers, disconnected switches, voltage and current transformers, post insulators, transformers and etc. To reduce the scale of the subsequent substation network model and also relieve the issue of the sparse reward in the learning process, the involved equipment components are grouped into eleven different macrocomponents according to equipment type, position, and interrelationship, as denoted in the grey box in Fig. 9.

After labeling the nodes with sequential numbers in Fig. 8, a directed graph-based presentation of the practical substation system with a total of 30 vertices and 43 edges $(E_1, E_2, ..., E_{43})$ can be derived, as presented in Fig. 9, where each edge denotes a specific predefined macrocomponent. In this regard, edges are removed from the graph when corresponding macrocomponents' states are damaged, and a corresponding adjacency matrix $A_{30\times30}$ of the substation system can be developed following the description in section 3.2 to produce the connectivity matrix $C_{30\times30}$ by Eq.(9) given the current macrocomponents' state vector $s = (s_1, s_2, ..., s_{43})$. Accordingly, the system functionality can be computed as explained below.

As defined in section 3.2, the system functionality, namely the maximum allowable transmission capacity, is computed by taking the minimum of P_I, P_T, P_O. Specifically for the practical substation case, Eq.(12) can be further modified and derived as Eq.(13).

$$
\begin{aligned}
F = f_F(s) &= \min\left(P_I, P_T, P_O\right) = \min\left(\sum_{i=1}^{3} TC_I(i), \sum_{i=1}^{2} TC_T(i), \sum_{i=1}^{6} TC_O(i)\right), \\
TC_M(i) &= SV_M(i) \times LC_M(i), \quad M \in \{I, P, O\}, \\
SV_M(i) &= [\sum C_{30\times30}(\mathbf{v_I}, v_M(i)) > 0] \times [\sum C_{30\times30}(v_M(i), \mathbf{v_O}) > 0],
\end{aligned}
\tag{13}
$$

in which the total power energy of each part in the substation, $P_M (M \in \{I, P, O\})$, is computed by summarizing the accessible transmission capacity of that part, TC_M; $LC_M(i)$ represents the load capacity of the $i-$th electrical bay in part M, as described in Fig. 8, while $SV_M(i)$ is a binary state variable indicating the accessibility of the $i-$th electrical bay in part M. In particular, source-load paths between the source nodes $\mathbf{v_I}$ and the load nodes $\mathbf{v_O}$ that pass through the concerned bay are subdivided into two links by treating a node in that bay as a breakpoint (denoted as $v_M(i)$). $SV_M(i)$ equals to "1" only if both links are intact. The links' integrity is determined based on the derived connectivity matrix $C_{30\times30}$, which records the electrical connectivity information of any two vertices within the substation network.

As an outcome, we can get the one-to-one mapping function between the system functionality and the macrocomponents state f_F. Moreover, the repair duration for each macrocomponent is again assumed to be the same with one time unit (one day) for simplicity and without loss of generality, and it can be conveniently replaced with other values for experiment, so that the designed resilience-based instant reward signal defined in Eq.(11) can also be obtained.

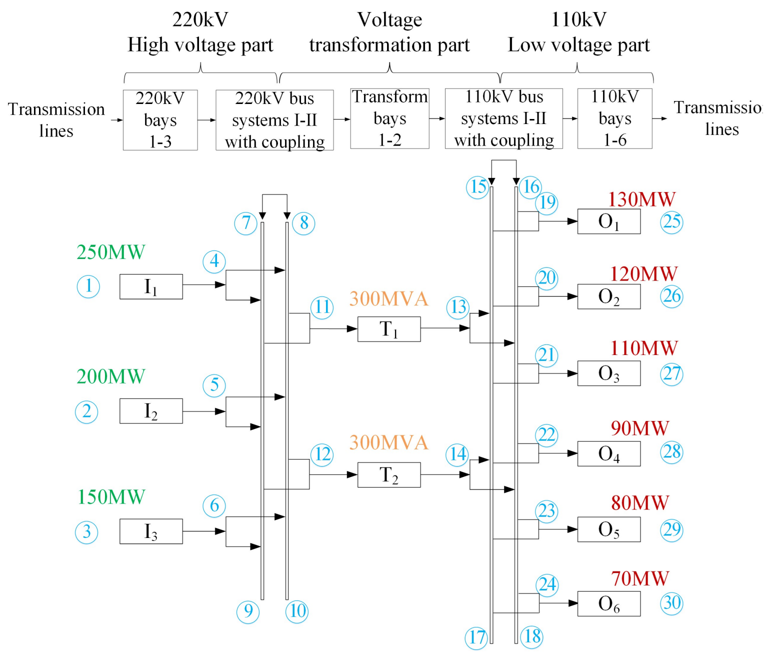

Fig. 8. Layout and power transmission path of the 220 kV step-down substation system (circles in blue are sequential numbered vertices; texts in green, orange, and red represent the load capacity of input bays, transformation bays, and output bays respectively)

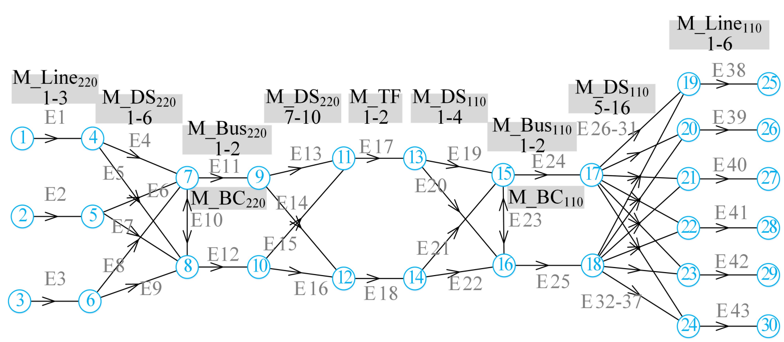

Fig. 9. Graph-based representation of the practical substation system with a total of 30 vertices and 43 edges that respectively represent specific macrocomponents

4.2 DRL experiments and training

The described substation recovery environment initialized with the most adverse damage scenario, where all the involved macrocomponents were damaged, is used to train the DRL-based decision support system for recovery optimization. Besides, a comprehensive comparison among the introduced DQN algorithm and its advanced variants, i.e., the DDQN, Duel DQN, and Duel DDQN, is conducted to evaluate their performance in solving this task.

The DDQN algorithm flowchart is offered in Fig. 10, which mainly modifies the DQN shown in Fig. 5 by decoupling the action selection and action evaluation using the policy network Q^p and Q^t,respectively. Additionally, for this complex system with high-dimensional state and action spaces, the greedy policy presented in Eq.(10) is modified by using the roulette wheel method to probabilistically select an action based on the estimated Q-values, as described by Eq.(14). This method can enhance the exploration-exploitation balance and improve learning stability, resulting in more effective and robust learning.

$$\begin{aligned} &P(a_i|s) = \frac{Q^p(s, a_i; \theta)}{\sum_{j=1}^{|\mathcal{A}|} Q^p(s, a_j; \theta)}, \\ &C_P(a_i|s) = \textstyle\sum_{k=1}^{i} P(a_k|s), \\ &C_P(a_{i-1}|s) < r \leq C_P(a_i|s), \end{aligned} \tag{14}$$

where $P(a_i|s)$ denotes the selection probability of repairing the $i-$th macrocomponent (a_i); $C_P(a_i|s)$ represents the cumulative probability up to and including action a_i; r is a random number uniformly distributed in the range [0,1], and the selected action should satisfy the above inequality conditions.

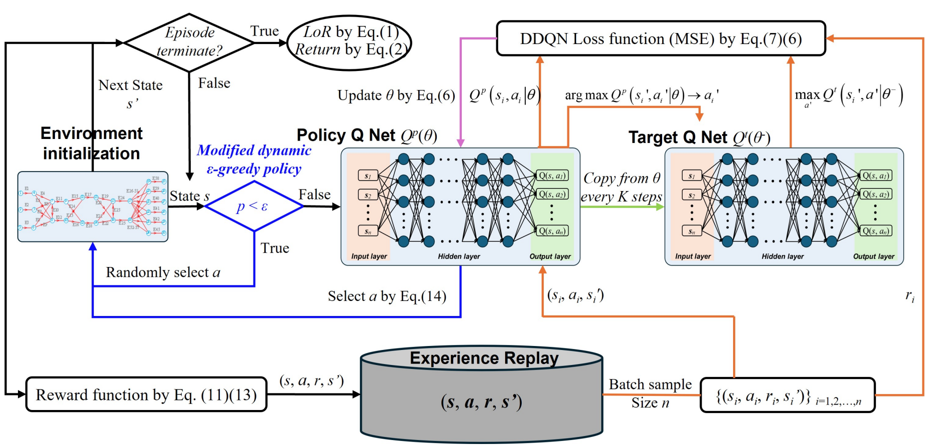

Fig. 10. DDQN algorithm flowchart to optimize the repair sequence of macrocomponents in the context of the practical substation system recovery environment

The Duel DQN and Duel DDQN advance their respective base algorithms (DQN and DDQN) by simply replacing the single Q-network structure with a dueling architecture without altering the fundamental algorithm flowcharts, as displayed in Fig. 11. The figure further displays the specific number of layers and neurons for the DNN-based agent in this experiment after parameter tuning. Particularly, we apply normalization after each fully connected layer with shared weights. After testing several architectures, we found that this setting yields the best results, likely due to the fact that the distributions after forward flow are preserved. Given this hypothesis, reusing norm layers alleviates the learning process by reducing the number of parameters to train. Other tested hyperparameters during the training experiments are listed in Table 2 and the value combination leading to the best performance is highlighted in bold.

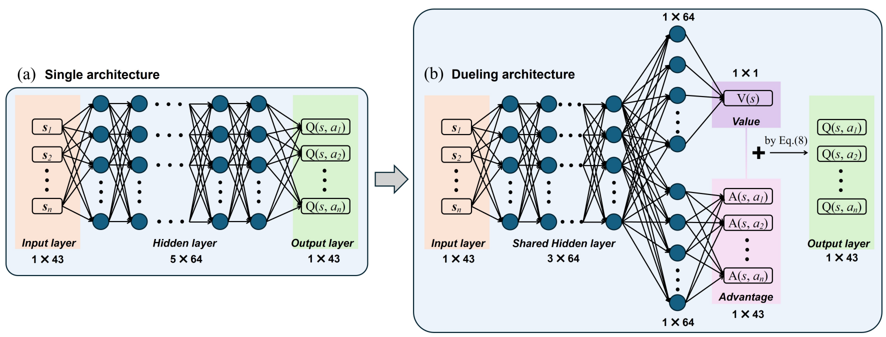

Fig. 11. Specific structures of (a) the single network and (b) the dueling network used in this experiment after parameter tuning

Table 2. Parameters for the training in the context of the practical substation system

parameter	**value**
Initial value of epsilon (ϵ_{start})	$[0.9, 0.95, \mathbf{1}]$
Final value of epsilon (ϵ_{end})	$[0.02, 0.01, 0.005, \mathbf{0.001}]$
Number of linearly decayed episodes(ϵ_{decay})	$[500, \mathbf{1000}, 2000]$
Size of repaly memory (D)	$[50000, \mathbf{100000}, 150000]$
Batch size (n)	$[64, \mathbf{128}, 256, 512]$
Discount factor (γ)	$[0.92, \mathbf{0.95}, 0.98]$
Learning rate (η)	$[0.01, 0.001, \mathbf{0.0001}, 0.00001]$
Target Q network update frequency (K)	$[50, \mathbf{100}, 200]$
Number of episodes for training (N)	$[\mathbf{10000}, 20000]$

Fig. 12 provides a comparison of the results for different Q-value based algorithms in our experiments in terms of the return reward and the resilience metric LoR over the number of episodes. As compared in Fig. 12(a), DDQN consistently observes the highest reward with less variance, followed by Duel DQN and Duel DDQN but with substantial variance, while DQN has the lowest performance in terms of final reward. Similarly in Fig. 12(b), DDQN shows the best performance in terms of resilience with the lowest and most stable LoR, followed by Duel DQN and Duel DDQN with slightly higher LoR values and more variance. DQN performs the worst, showing even higher LoR values in the end. Table 3 further compares the best LoR outcomes during training for the four algorithms. DDQN achieves the lowest LoR value of 9860 MW·day, an 18.3% improvement over the DQN baseline of 12070 MW·day. Duel DQN and Duel DDQN show improvements with the values of 11110 MW·day (8.0% reduction) and 11370 MW·day (5.8% reduction), respectively. Overall, DDQN outperforms the other algorithms in both the designed reward signal and ultimate resilience metric, rendering this the most effective in the given experimental setup. By saving this top-performing agent model, it can be readily deployed for future decision-making on recovery optimization, leveraging its learned strategies to enhance system resilience under any stochastic damage scenario as shown below.

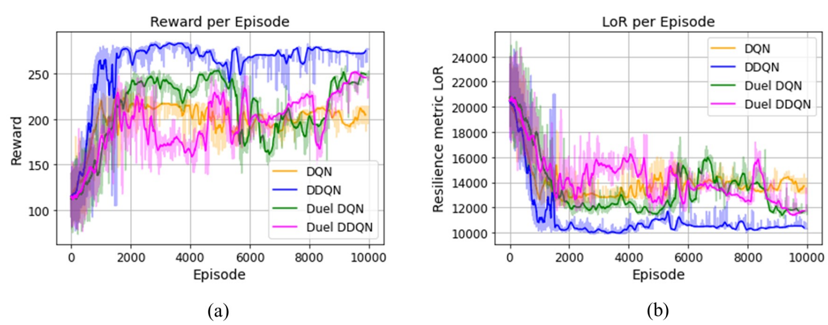

Fig. 12. Comparison for different Q-value based algorithms in terms of the evolution of (a) Reward over training episodes; (b) LoR over training episodes

Table 3. Comparison of the four algorithms in terms of the best LoR outcomes during the training

Algorithm	DQN	DDQN	Duel DQN	Duel DDQN
Best LoR(MW·day)	12070	9860	11110	11370
Variation(%)	base line	-18.3	-8.0	-5.8

4.3 Performance evaluation and discussion

Fig. 13 compares the recovery performance in terms of the resulting resilience curves of the practical substation system between the conventional exhaustive or GA-based search methods and the trained DRL model across various initial damage scenarios. Subfigures (a) through (d) illustrate random damage scenarios with increasing severity, which are generated here by randomly setting a total of 8, 16, 32, and 40 damaged components respectively [65]. While subfigure (e) depicts the training scenario where all components are damaged. The left panels in each subfigure present the post-disaster condition of the substation network with damaged components marked in red, while the right panels display the resilience curves comparing the best recovery performance from traditional methods (green and orange solid lines) against the DRL-based approach (blue dashed lines). The grey lines, represent the performance of multiple GA runs initiated with different random seeds, illustrating notable variability in the GA performance. Notably, as the number of damaged components increases, the performance variability also increases, indicating that the robustness of the traditional GA-based repair sequence optimization method diminishes with greater damage severity. In contrast, the trained DRL model demonstrates robust performance and consistently yields results that are equal to or even better than the best outcomes from traditional methods across all scenarios. Additionally, the substation system's redundancy design implies that not all damaged components need to be repaired to restore system functionality in emergency situations. It has been observed that the trained DRL agent can learn this aspect and effectively account for component interdependencies in its repair strategies, as shown in the appendix. The corresponding resilience metric LoR and the required computational time by different methods for both the training damage scenario and the new random damage scenarios are listed in Table 4. As compared on the training damage scenario, the DRL-based method achieves better LoR value (i.e., 9920 MW·day versus 10560 MW·day) with around four times less computational time (i.e., 5687 seconds against 23120 seconds) compared to the GA-based method. The advantages are even more obvious when applying the trained model to some random severe damage scenarios (e.g., $DS3$ and $DS4$). This demonstrates the efficiency of the DRL-based decision framework in optimizing recovery sequences and its superior capability in achieving high system resilience. Furthermore, the DRL-based model trained on the worst case can also leverage its learned policy to provide a system resilience-enhanced recovery solution for any stochastic damage scenario in a near real-time manner, which is quite valuable in guiding emergency response in the face of future disasters.

5 Conclusions

In this study, we develop a DRL-based model to optimize the post-disaster recovery planning of electrical substation systems with the aim of enhancing resilience as quantified in terms of the lack-of-resilience metric (LoR). This model addresses the limitations of existing optimization methods and leverages deep Q-learning algorithms to learn optimal recovery strategies by mapping system states to repair actions that maximize long-term recovery outcomes in a global

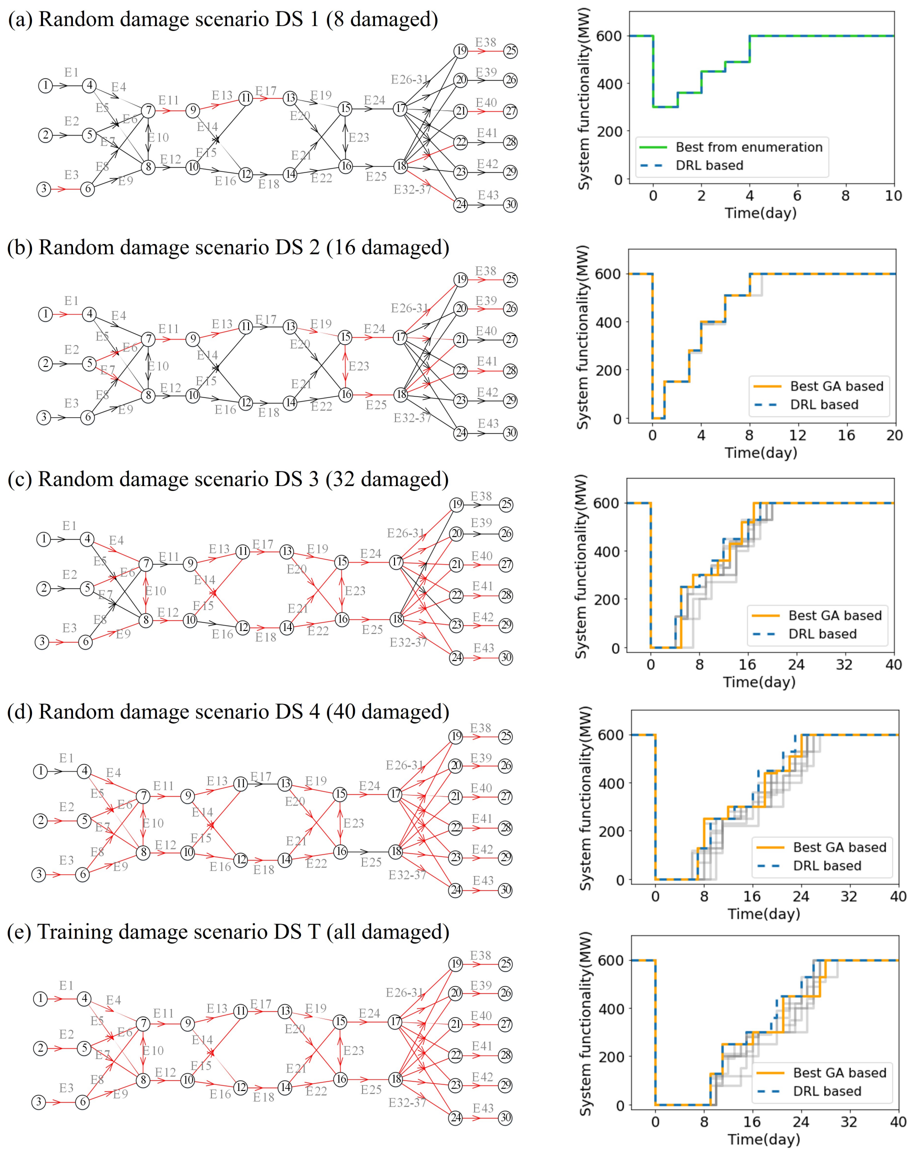

Fig. 13. Recovery performance comparison in terms of the resulting resilience curves between the traditional exhaustive or GA-based search and the trained DRL model for (a)(b)(c)(d) some random damage scenarios; and (e) the training damage scenario (Green and orange solid lines highlight the best resilience outcome with the minimum LoR among the others denoted in gray that are obtained from the traditional methods; blue dashed lines represent the results generated from the trained DRL model)

Table 4. Comparison of the traditional recovery optimization methods and the introduced DRL-based decision support framework in terms of the *LoR* value and computational cost on different initial damage scenarios

Method	**Performance index**	**Initial Damage Scenario**				
		DS T	**DS 1**	**DS 2**	**DS 3**	**DS 4**
Enumeration or GA-based	Best LoR (MW·day)	10560	800	2400	5880	8670
	Time cost (s)	23120	1373	3487	11170	17389
DRL-based	LoR (MW·day)	9920	800	2400	5740	8420
	Time cost (s)	5687	0.02	0.04	0.09	0.13

perspective. The key contributions and findings of our study are summarized as follows:

1. Resilience-augmented sequential decision-making framework based on graph: we model the system network with a graph-based representation and formulate the recovery process as a sequential decision-making problem, where the DRL agent learns to identify which damaged components in the graph representation to repair based on the available resource and system state at each time step. This is achieved by performing recovery trials and interacting with a simulated substation environment, reducing the need for extensive hard-to-obtain labeled data in state-of-art methods. The graph-based representation better reflects the actual network topology, enabling the DRL agent to learn from both local and global interdependencies, leading to more accurate and scalable decision-making in dynamic recovery scenarios. By explicitly incorporating resilience metric into the reward function, the framework optimizes not only immediate functionality gain but also long-term recovery resilience, resulting in a more balanced recovery strategy that can maximize system resilience in a global perspective.

2. Comparison of DRL Architectures and Use of Case-specific Enhanced Update Rules: we conduct a thorough comparison of different deep Q-learning algorithms, including vanilla Deep Q-Networks (DQN), Double DQN (DDQN), Duel DQN, and Duel DDQN. In particular, we apply several techniques to enhance algorithm performance, such as adopting an action mask to penalize invalid repair actions, modifying the greedy action selection policy by the roulette wheel method based on the estimated action Q-values, and conducting normalization after each fully connected layer in the agent with shared weights. These practices are shown to yield improved exploration-exploitation balance and improved convergence performance. Our results demonstrate that DDQN outperforms other algorithms in obtaining the best system-level resilience outcome during training.

3. Superior Performance, Robustness, and Adaptability: we further compare the performance of the best DDQN model with multiple GA-based optimization runs on the worst-case training damage scenario, where all the involved components are assumed to be damaged. This provides the DRL agent with a broader overview on the substation recovery environment. The DRL-based approach achieves a more robust and superior *LoR* by 6% with four times less training time compared to the best GA-based outcome. Furthermore, the DRL

model trained on the worst-case scenario showed excellent adaptability, yielding results that are equal to or even better than the best GA-based outcomes across various unforeseen damage scenarios in near real-time. This underscores the potential of the pre-trained DRL-based model to provide real-time decision support in the face of unexpected disasters without requiring time-costly retraining.

This work contributes to the field of disaster emergency decision-making by introducing a DRL-based framework that provides a robust and efficient solution for optimizing post-disaster recovery of substation system in a near-real time manner, while also accounting for the redundancy, dynamic and interconnected nature of that system. The findings highlight the potential of DRL to revolutionize disaster recovery planning, paving the way for more resilient and sustainable substation systems in the face of future disasters.

Future research will explore the application of our approach to other types of infrastructure systems and disasters, as well as the integration of real-time data and partial information to further improve recovery strategies. The algorithm capitalises on the hypothesis of the total failure of all equipment within the substation. Although this assumption enables the DL approach to derive more generalized principles for recovery planning strategies, the learning conditions are rather stringent, and analyzing all potential resilience pathways becomes computationally consuming and challenging to converge during training. Multi-environment DRL can use parallel autonomous simulations to expedite data and experience accumulation, alleviating the drawback of single environment approaches [47, 26]. Also, recent works on the use of graph neural networks (GNNs) in the architecture of the DQN reveal the versatility of these DNNs to learn patterns efficiently in highly irregular and complex domains and connectivity grids, being more efficient than conventional methods [67, 53]. As a result, next steps should follow this direction to further exploit the benefits of graph formulations [69].

Acknowledgments. The research was conducted at the Singapore-ETH Centre, which was established collaboratively between ETH Zurich and the National Research Foundation Singapore, and CNRS@CREATE through the DESCARTES program, both research supported by the National Research Foundation, Prime Minister's Office, Singapore under its Campus for Research Excellence and Technological Enterprise (CREATE) programme. F.C. also acknowledges the support of the Chimera RTE research chairs at Arts et Metiers Institute of Technology (ENSAM).

Disclosure of Interests. The authors have no competing interests to declare that are relevant to the content of this article.

References

[1] Harry R Lewis. "Michael R. ΠGarey and David S. Johnson. Computers and intractability. A guide to the theory of NP-completeness. WH Freeman and Company, San Francisco1979, x+ 338 pp." In: *The Journal of Symbolic Logic* 48.2 (1983), pp. 498–500.

[2] Michel Bruneau et al. “A framework to quantitatively assess and enhance the seismic resilience of communities”. In: *Earthquake spectra* 19.4 (2003), pp. 733–752.
[3] Ningxiong Xu et al. “Optimizing scheduling of post-earthquake electric power restoration tasks”. In: *Earthquake engineering & structural dynamics* 36.2 (2007), pp. 265–284.
[4] Devanandham Henry and Jose Emmanuel Ramirez-Marquez. “Generic metrics and quantitative approaches for system resilience as a function of time”. In: *Reliability Engineering & System Safety* 99 (2012), pp. 114–122.
[5] Isaac Hernandez-Fajardo and Leonardo Dueñas-Osorio. “Probabilistic study of cascading failures in complex interdependent lifeline systems”. In: *Reliability Engineering & System Safety* 111 (2013), pp. 260–272.
[6] Alexis Kwasinski et al. “Performance of electric power systems in the 2010–2011 Christchurch, New Zealand, earthquake sequence”. In: *Earthquake Spectra* 30.1 (2014), pp. 205–230.
[7] Min Ouyang and Leonardo Duenas-Osorio. “Multi-dimensional hurricane resilience assessment of electric power systems”. In: *Structural Safety* 48 (2014), pp. 15–24.
[8] Min Ouyang and Kun Yang. “Does topological information matter for power grid vulnerability?” In: *Chaos: An Interdisciplinary Journal of Nonlinear Science* 24.4 (2014).
[9] Paolo Franchin and Francesco Cavalieri. “Probabilistic assessment of civil infrastructure resilience to earthquakes”. In: *Computer-Aided Civil and Infrastructure Engineering* 30.7 (2015), pp. 583–600.
[10] Volodymyr Mnih et al. “Human-level control through deep reinforcement learning”. In: *nature* 518.7540 (2015), pp. 529–533.
[11] Oriol Vinyals, Meire Fortunato, and Navdeep Jaitly. “Pointer networks”. In: *Advances in neural information processing systems* 28 (2015).
[12] Gianluca Pescaroli and David Alexander. “Critical infrastructure, panarchies and the vulnerability paths of cascading disasters”. In: *Natural Hazards* 82 (2016), pp. 175–192.
[13] Hado Van Hasselt, Arthur Guez, and David Silver. “Deep reinforcement learning with double q-learning”. In: *Proceedings of the AAAI conference on artificial intelligence*. Vol. 30. 1. 2016.
[14] Ziyu Wang et al. “Dueling network architectures for deep reinforcement learning”. In: *International conference on machine learning*. PMLR. 2016, pp. 1995–2003.
[15] Enrico Zio. “Challenges in the vulnerability and risk analysis of critical infrastructures”. In: *Reliability Engineering & System Safety* 152 (2016), pp. 137–150.
[16] Weili Zhang, Naiyu Wang, and Charles Nicholson. “Resilience-based post-disaster recovery strategies for road-bridge networks”. In: *Structure and Infrastructure Engineering* 13.11 (2017), pp. 1404–1413.

[17] Vincent François-Lavet et al. "An introduction to deep reinforcement learning". In: *Foundations and Trends® in Machine Learning* 11.3-4 (2018), pp. 219–354.
[18] Jürgen Hackl, Bryan T Adey, and Nam Lethanh. "Determination of near-optimal restoration programs for transportation networks following natural hazard events using simulated annealing". In: *Computer-Aided Civil and Infrastructure Engineering* 33.8 (2018), pp. 618–637.
[19] Richard S Sutton and Andrew G Barto. *Reinforcement learning: An introduction*. MIT press, 2018.
[20] Charalampos P Andriotis and Konstantinos G Papakonstantinou. "Managing engineering systems with large state and action spaces through deep reinforcement learning". In: *Reliability Engineering & System Safety* 191 (2019), p. 106483.
[21] Ian M Cavalcante et al. "A supervised machine learning approach to data-driven simulation of resilient supplier selection in digital manufacturing". In: *International Journal of Information Management* 49 (2019), pp. 86–97.
[22] Yi-Ping Fang and Giovanni Sansavini. "Optimum post-disruption restoration under uncertainty for enhancing critical infrastructure resilience". In: *Reliability Engineering & System Safety* 185 (2019), pp. 1–11.
[23] Beakcheol Jang et al. "Q-learning algorithms: A comprehensive classification and applications". In: *IEEE access* 7 (2019), pp. 133653–133667.
[24] Chaitanya K Joshi, Thomas Laurent, and Xavier Bresson. "An efficient graph convolutional network technique for the travelling salesman problem". In: *arXiv preprint arXiv:1906.01227* (2019).
[25] Nguyen Cong Luong et al. "Applications of deep reinforcement learning in communications and networking: A survey". In: *IEEE communications surveys & tutorials* 21.4 (2019), pp. 3133–3174.
[26] Jean Rabault and Alexander Kuhnle. "Accelerating deep reinforcement learning strategies of flow control through a multi-environment approach". In: *Physics of Fluids* 31.9 (2019).
[27] Navid Ahmadian et al. "A quantitative approach for assessment and improvement of network resilience". In: *Reliability Engineering & System Safety* 200 (2020), p. 106977.
[28] Sotirios A Argyroudis et al. "Resilience assessment framework for critical infrastructure in a multi-hazard environment: Case study on transport assets". In: *Science of the Total Environment* 714 (2020), p. 136854.
[29] Maria Koliou et al. "State of the research in community resilience: Progress and challenges". In: *Sustainable and resilient infrastructure* 5.3 (2020), pp. 131–151.
[30] Wei Liu and Zhaoyang Song. "Review of studies on the resilience of urban critical infrastructure networks". In: *Reliability Engineering & System Safety* 193 (2020), p. 106617.

[31] Wei Liu et al. "Recovery-based seismic resilience enhancement strategies of water distribution networks". In: *Reliability Engineering & System Safety* 203 (2020), p. 107088.

[32] Hossein Nasrazadani and Mojtaba Mahsuli. "Probabilistic framework for evaluating community resilience: integration of risk models and agent-based simulation". In: *Journal of Structural Engineering* 146.11 (2020), p. 04020250.

[33] Mohammad Hossein Oboudi et al. "A systematic method for power system hardening to increase resilience against earthquakes". In: *IEEE Systems Journal* 15.4 (2020), pp. 4970–4979.

[34] Neetesh Sharma, Armin Tabandeh, and Paolo Gardoni. "Regional resilience analysis: A multiscale approach to optimize the resilience of interdependent infrastructure". In: *Computer-Aided Civil and Infrastructure Engineering* 35.12 (2020), pp. 1315–1330.

[35] Lijuan Shen et al. "Large-scale systems resilience: A survey and unifying framework". In: *Quality and Reliability Engineering International* 36.4 (2020), pp. 1386–1401.

[36] Wenjuan Sun, Paolo Bocchini, and Brian D Davison. "Resilience metrics and measurement methods for transportation infrastructure: The state of the art". In: *Sustainable and Resilient Infrastructure* 5.3 (2020), pp. 168–199.

[37] Charalampos P Andriotis and Konstantinos G Papakonstantinou. "Deep reinforcement learning driven inspection and maintenance planning under incomplete information and constraints". In: *Reliability Engineering & System Safety* 212 (2021), p. 107551.

[38] Mateusz Iwo Dubaniowski and Hans Rudolf Heinimann. "Framework for modeling interdependencies between households, businesses, and infrastructure system, and their response to disruptions—application". In: *Reliability Engineering & System Safety* 212 (2021), p. 107590.

[39] Craig Poulin and Michael B Kane. "Infrastructure resilience curves: Performance measures and summary metrics". In: *Reliability Engineering & System Safety* 216 (2021), p. 107926.

[40] Inkyung Sung, Bongjun Choi, and Peter Nielsen. "On the training of a neural network for online path planning with offline path planning algorithms". In: *International Journal of Information Management* 57 (2021), p. 102142.

[41] Nikola Bešinović, Raphael Ferrari Nassar, and Christopher Szymula. "Resilience assessment of railway networks: Combining infrastructure restoration and transport management". In: *Reliability Engineering & System Safety* 224 (2022), p. 108538.

[42] Nikola Blagojević and Božidar Stojadinović. "A demand-supply framework for evaluating the effect of resource and service constraints on community disaster resilience". In: *Resilient Cities and Structures* 1.1 (2022), pp. 13–32.

[43] Xudong Fan, Xijin Zhang, and Xiong Yu. “A graph convolution network-deep reinforcement learning model for resilient water distribution network repair decisions”. In: *Computer-Aided Civil and Infrastructure Engineering* 37.12 (2022), pp. 1547–1565.

[44] Mohammad Mehdi Hosseini and Masood Parvania. “Resilient Operation of Distribution Grids Using Deep Reinforcement Learning”. In: *IEEE Transactions on Industrial Informatics* 18.3 (2022), pp. 2100–2109. DOI: 10.1109/TII.2021.3086080.

[45] Huangbin Liang and Qiang Xie. “Resilience-based sequential recovery planning for substations subjected to earthquakes”. In: *IEEE Transactions on Power Delivery* 38.1 (2022), pp. 353–362.

[46] Huangbin Liang et al. “Seismic risk analysis of electrical substations based on the network analysis method”. In: *Earthquake Engineering & Structural Dynamics* 51.11 (2022), pp. 2690–2707.

[47] Mirco Mutti, Mattia Mancassola, and Marcello Restelli. “Unsupervised reinforcement learning in multiple environments”. In: *Proceedings of the AAAI Conference on Artificial Intelligence*. Vol. 36. 7. 2022, pp. 7850–7858.

[48] Xing Pan et al. “Resilience model and recovery strategy of transportation network based on travel OD-grid analysis”. In: *Reliability Engineering & System Safety* 223 (2022), p. 108483.

[49] Alejandro del Real Torres et al. “A review of deep reinforcement learning approaches for smart manufacturing in industry 4.0 and 5.0 framework”. In: *Applied Sciences* 12.23 (2022), p. 12377.

[50] Alaa Selim et al. “Deep Reinforcement Learning for Distribution System Restoration Using Distributed Energy Resources and Tie-Switches”. In: (Oct. 2022). DOI: 10.1109/PESGM48719.2022.9916740. URL: https://www.osti.gov/biblio/1908959.

[51] Armin Tabandeh, Neetesh Sharma, and Paolo Gardoni. “Uncertainty propagation in risk and resilience analysis of hierarchical systems”. In: *Reliability Engineering & System Safety* 219 (2022), p. 108208.

[52] Kazuaki Akashi et al. “Deep Reinforcement Learning for Network Service Recovery in Large-Scale Failures”. In: *2023 19th International Conference on Network and Service Management (CNSM)*. 2023, pp. 1–5. DOI: 10.23919/CNSM59352.2023.10327883.

[53] Xudong Fan et al. “A deep reinforcement learning model for resilient road network recovery under earthquake or flooding hazards”. In: *Journal of Infrastructure Preservation and Resilience* 4.1 (2023), p. 8.

[54] Hamed Hafeznia and Božidar Stojadinović. “ResQ-IOS: An iterative optimization-based simulation framework for quantifying the resilience of interdependent critical infrastructure systems to natural hazards”. In: *Applied Energy* 349 (2023), p. 121558.

[55] Yucheng Hao et al. “Improving resilience of high-speed train by optimizing repair strategies”. In: *Reliability Engineering & System Safety* 237 (2023), p. 109381.

[56] Huangbin Liang et al. "Seismic resilience assessment and improvement framework for electrical substations". In: *Earthquake Engineering & Structural Dynamics* 52.4 (2023), pp. 1040–1058.

[57] Paolo Trucco and Boris Petrenj. "Characterisation of resilience metrics in full-scale applications to interdependent infrastructure systems". In: *Reliability Engineering & System Safety* 235 (2023), p. 109200.

[58] Giacomo Arcieri et al. "POMDP inference and robust solution via deep reinforcement learning: An application to railway optimal maintenance". In: *Machine Learning* (2024), pp. 1–29.

[59] Abdullah M. Braik and Maria Koliou. "A digital twin framework for efficient electric power restoration and resilient recovery in the aftermath of hurricanes considering the interdependencies with road network and essential facilities". In: *Resilient Cities and Structures* 3.3 (2024), pp. 79–91. ISSN: 2772-7416. DOI: `https://doi.org/10.1016/j.rcns.2024.07.004`. URL: `https://www.sciencedirect.com/science/article/pii/S2772741624000310`.

[60] Mehmet Gök. "Dynamic path planning via Dueling Double Deep Q-Network (D3QN) with prioritized experience replay". In: *Applied Soft Computing* 158 (2024), p. 111503.

[61] PC Haritha and MVLR Anjaneyulu. "Comparison of topological functionality-based resilience metrics using link criticality". In: *Reliability Engineering & System Safety* 243 (2024), p. 109881.

[62] Roshni Anna Jacob et al. "Real-time outage management in active distribution networks using reinforcement learning over graphs". In: *Nature Communications* 15.1 (June 2024), p. 4766. ISSN: 2041-1723. DOI: `10.1038/s41467-024-49207-y`. URL: `https://doi.org/10.1038/s41467-024-49207-y`.

[63] Daniel Koutas, Elizabeth Bismut, and Daniel Straub. "An investigation of belief-free DRL and MCTS for inspection and maintenance planning". In: *Journal of Infrastructure Preservation and Resilience* 5.1 (2024), p. 6.

[64] Diya Li et al. "A reinforcement learning-based routing algorithm for large street networks". In: *International Journal of Geographical Information Science* 38.2 (2024), pp. 183–215.

[65] Huangbin Liang and Qiang Xie. "Probabilistic seismic risk analysis of electrical substations considering equipment-to-equipment seismic failure correlations". In: *Reliability Engineering & System Safety* (2024), p. 110588.

[66] Feng Wang et al. "A multi-stage quantitative resilience analysis and optimization framework considering dynamic decisions for urban infrastructure systems". In: *Reliability Engineering & System Safety* 243 (2024), p. 109851.

[67] Sen Yang et al. "Multi-agent deep reinforcement learning based decision support model for resilient community post-hazard recovery". In: *Reliability Engineering & System Safety* 242 (2024), p. 109754.

[68] Wangxin Zhang et al. “Resilience-based post-earthquake restoration scheduling for urban interdependent transportation-electric power network”. In: *Structure and Infrastructure Engineering* (2024), pp. 1–18.

[69] XU HAN et al. “Predicting Physics in Mesh-reduced Space with Temporal Attention”. In: *International Conference on Learning Representations*.

6 Appendix

This section provides the repair sequence determined by the trained DRL model and the resulting graph-based network configurations over recovery time for the practical substation across various initial damage scenarios. As presented, the trained DRL agent can effectively account for component interdependencies and redundancy in the substation network system, and derive smart repair plan solution to efficiently restore system's functionality by prioritizing the repair of the critical components for different damaged scenarios without the need for retraining.

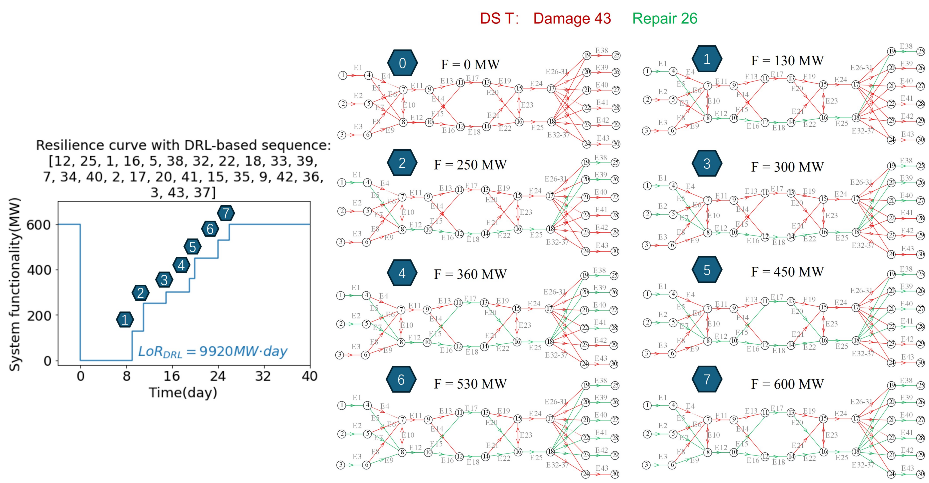

Fig. 14. The repair sequence determined by the DRL-based model on the worst-case damage scenario and the resulting graph-based network configurations over recovery time

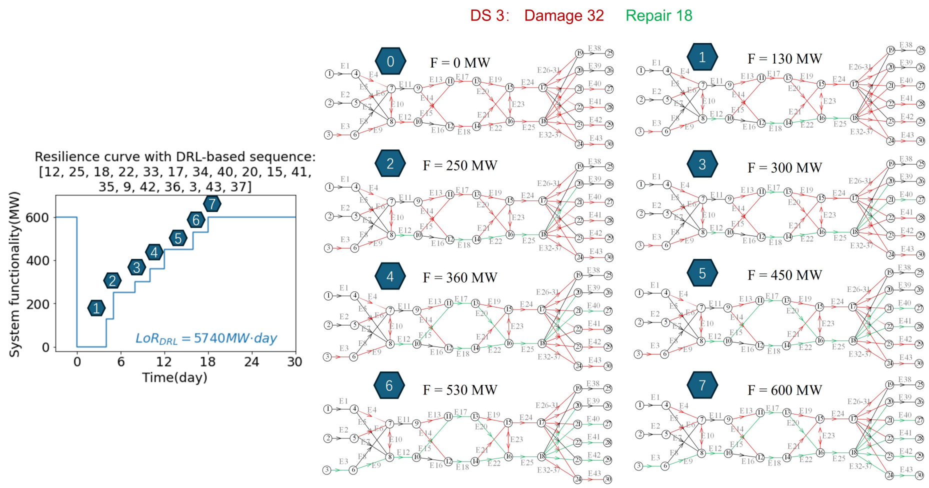

Fig. 15. The repair sequence determined by the DRL-based model on the DS3 damage scenario and the resulting graph-based network configurations over recovery time

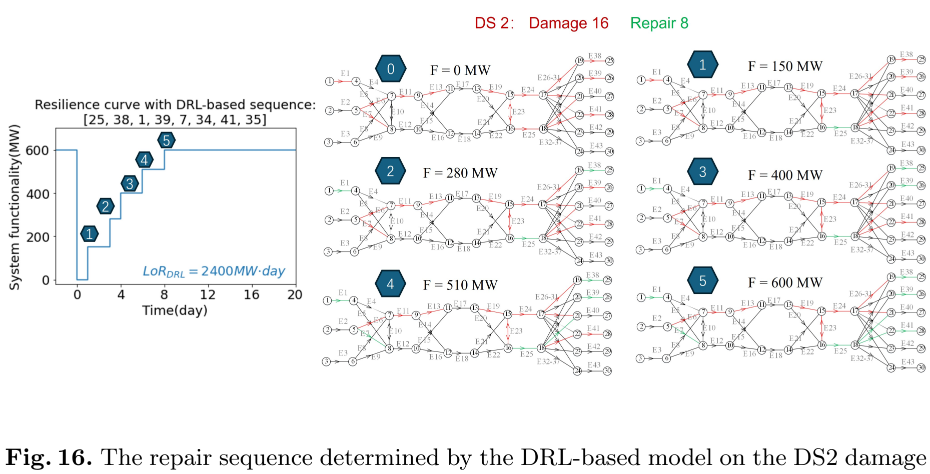

Fig. 16. The repair sequence determined by the DRL-based model on the DS2 damage scenario and the resulting graph-based network configurations over recovery time

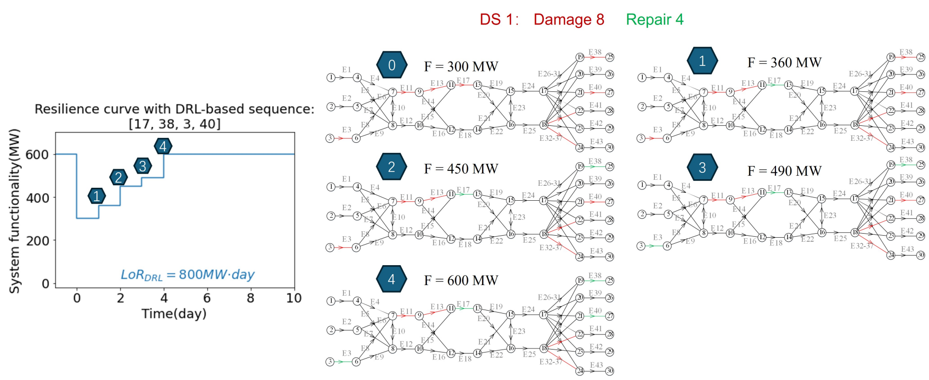

Fig. 17. The repair sequence determined by the DRL-based model on the DS1 damage scenario and the resulting graph-based network configurations over recovery time